Materials Today Communications 21 (2019) 100691

Contents lists available at ScienceDirect

Materials Today Communications

journal homepage: www.elsevier.com/locate/mtcomm

Corrosion inhibition of mild steel using binary mixture of sesame and castor oil in brine solution

Daniel T. Oyekunle[a,*], Tomiwa I. Oguntade[b], Christiana S. Ita[b], Temiloluwa Ojo[b], Oyinkepreye D. Orodu[b]

[a] Department of Chemical Engineering, College of Engineering, Covenant University, Nigeria
[b] Department of Petroleum Engineering, College of Engineering, Covenant University, Nigeria

ARTICLE INFO

Keywords:
Sesame oil
Castor oil
Mild steel
Weight loss
Polarization

ABSTRACT

Binary mixture of sesame and castor oil has been investigated as a corrosion inhibitor for mild steel in brine solutions by weight loss, polarization techniques and scanning electron microscopy (SEM) analysis. Gas Chromatography–Mass Spectroscopy (GC–MS) analysis showed the presence of unsaturated compounds like oleic, steric and palmitic acid which are responsible for the corrosion inhibitory properties of the binary mixture. Optimum inhibition efficiency of 86.2% was predicted by Minitab 17 statistical software using the weight loss method at 0.79 M brine concentration, 22.1 mg/ L concentration of binary inhibitor and at a time period of 14 days. Tafel polarization plots affirm that binary mixture of sesame and castor oil acts as an effective mixed-type inhibitor in moderately low concentrations while it also acts as anodic and cathodic inhibitors in high concentration of brine. The results of the SEM analysis also indicate the inhibition efficiency of the binary mixture of mild steel.

1. Introduction

Corrosion is an irreversible and rapid degradation of metal and alloy with the environment through an electrochemical or chemical reaction. Corrosion is a destructive phenomenon that affects the beauty of an object, and often times causing structural failure. Corrosion of metals affects its impact on the environment and its economic value [1]. It causes a huge waste of metallic materials which results in high economic losses globally. As a consequence of this, corrosion has led to significant industrial and academic awareness. Corrosion is a worldwide problem, negatively affecting the advancement of developed and developing countries. According to a study by the National Association of Corrosion Engineers (NACE), in 2011, more than US $2.2 trillion was spent on corrosion. The cost of corrosion in India was estimated to be above US $100 billion, also about US $9.6 billion was expended on corrosion in South Africa. It was reported that the amount spent on corrosion can be reduced by 35% using the prevailing methods of preventing corrosion [2].

Typically, erosion is the degradation of metallic materials by physical factors but corrosion is restricted to harmful attacks on metals only [3]. Most non-metallic materials are susceptible to deterioration by chemical reaction with the immediate environment. Often times, non-metallic materials deteriorate as a result of the chemical reaction with the surroundings, for instance, cracks and bulges are observed in plastics, eroding of the outer layer is observed on granite surfaces, split observed on wood and leaching of Portland. Corrosion is restricted to destructive attack on metals by electrochemical and /or chemical attack [2]. However, a frequent and effective means of protecting metallic substrates from corrosion occurs when organic coatings are applied. Organic coatings confer metal protection by the creation of a protective layer against oxygen so as to reduce the corrosion rate by lowering the presence of corrosion-causing factors like water hydrogen and oxygen ion on metal surfaces. Although, as a result of the permissiveness of organic coatings to water and oxygen, some active ingredients such as inorganic additives are added to these inhibitors to further hinder the corrosion rate especially once the protective covering has been breached [4,5].

Different types of organic compounds have been applied as an inhibitor to form organic coatings. Often times, organic compounds possess a significant influence on the rate at which adsorption occurs on a metal surface, hence they can effectively inhibit corrosion. The efficiency of organic inhibitors is due to the existence of polar functions with S, O or N atoms in the molecules, π electrons, and heterocyclic compounds. Also, the polar function is referred to as the center for the

* Corresponding author.
E-mail address: daniel.oyekunle@covenantuniversity.edu.ng (D.T. Oyekunle).

https://doi.org/10.1016/j.mtcomm.2019.100691
Received 26 July 2019; Received in revised form 6 October 2019; Accepted 8 October 2019
Available online 13 October 2019

inception of the adsorption process [6]. Most synthetic organic inhibitors have several hazardous effects and controlled environmental regulations, which had made researchers focus on developing cheap, non-toxic and environmentally favorable natural products as corrosion inhibitors. These natural organic compounds can be synthesized or extracted from a medicinal plant, aromatic herbs, and spices. Plants extracts are seen as a remarkable source of chemical compounds that can be extracted easily at a low cost and are biodegradable in nature [7]. The use of natural products extracted from leaves, seeds, and roots of plants as a corrosion inhibitor has been documented in the literature [8–11].

Numerous extracts from plants have been used as corrosion inhibitors this includes *Hibiscus sabdariffa, Azadirachta indica, Telferia occidentalis, Occimum viridis and Garcinia kola* extract [12]. Other plant extracts that have been used are succinic acid [13], ascorbic acid [14], aminoacids [15], Pennyroyal oil [16], *Justicia gendarussa* [7] and caffeic acid [17]. In previous studies, castor oil has been used as a corrosion inhibitor on mild steel [18–20] as well as *Sesame oil* [21,22]. Castor oil has proved to be an efficient inhibitor as a result of the presence of a functional group with 12C. The existence of OH groups in fatty acid chains makes the oil unusually polar [19]. As a result of this inhibitive nature, this study was performed to combine the corrosion inhibitive property of both oils (sesame and castor oil) in a binary mixture on mild steel. The morphology and compositions of the precipitated film on the mild steel surface in brine solutions containing different concentrations of the binary inhibitor (sesame and castor oil) were studied by SEM and FT-IR analysis. Polarization tests were also carried out to examine corrosion inhibition effects at different immersion times.

Statistical models such as Artificial Neural Network (ANN) and Response Surface Methodology (RSM) have been applied to optimize various processes in numerous fields. [23–25]. Response surface methodology is a mathematical and statistical tool used to study individual and interactional effects of variables on responses and is mostly fitted by polynomial equations such as quadratic, cubic or higher-order functions. Box Behnken design (BBD) was selected from other RSM designs as a result of its efficiency, feasibility, simplicity and also to reduce the number of test runs required compared to other RSM designs. On the other hand, a computational technique such as ANN imitates biological neural systems like the human brain. RSM and ANN are computer software programs designed to model the correlation between the independent and dependent variables and are proficient in the modeling of non-linear and complex relationships directly from raw data. The benefit of using ANNs is its capacity to control complex, noisy, incomplete and less constructive data and its ability of parallel processing [25].

In this study, response surface methodology (RSM) Box-Behnken design was used to design experimental sets and to investigate the effects of main and interaction of process variables such as concentration of inhibitor, concentration of the corrosive medium (brine), and time using binary mixture of sesame and castor oil, and the same sets of experimental data was applied for training artificial neural network. The results acquired from both models (RSM and ANN) were compared to ensure better predictability of inhibition efficiency of the binary inhibitor (sesame and castor oil) on mild steel in brine solutions.

2. Experimental procedures

2.1. Materials

2.1.1. Preparation of plant extract and coupon preparation

Sesame and castor oil were obtained from Lagos State, Nigeria. Both oils (sesame and castor oil) were viscous, the sesame oil was a dark brown liquid while the castor oil was a light yellow liquid. Equal volumes of both oils were used throughout this experiment. Mild steel coupons (Mn = 0.03; Cr = 0.012; C = 0.253; S = 0.024; P = 0.013; Si = 0.12; and remainder Fe) of dimensions 20 × 20 x 3 mm size were used for weight loss measurements and polarization studies. Prior to the experiments, the coupons were polished with 600 grade of emery papers. They were immersed in acetone for 20 min to remove grease, washed with distilled water and dried in air before immersing in the corrosion medium.

2.1.2. Gas chromatography- mass spectrometry (GCMS)

8 µl of the binary inhibitor with equal volumes of sesame and castor oil were sonicated using n-hexane and analyzed by GCMS-QP2010 Plus Shimadzu, Japan equipped with electron impact ionization mass spectrometer. The oven temperature was programmed at 70–280°C at a linear velocity of 49.2 cm/sec and held for a hold-up time of 5 min. Other operating conditions are: split ratio 20.0, detector temperature 280 ^{0}C, injector temperature 250 ^{0}C and Helium (99.99%) was used as the carrier gas.

2.1.3. Fourier transform infrared spectroscopy (FTIR)

FTIR instrument, Shimadzu FTIR-8400S was used to perform structural characterization of the binary inhibitor. The functional groups were analyzed in the range of 750 – 4000 cm^{-1} (wavenumbers), and established by correlation with the standard peak placement of the groups.

2.2. Methods

2.2.1. BBD and ANN optimization and design of experiments using weight loss method

Box-Behnken Design (BBD) and Artificial Neural Network (ANN) were applied to give a precise prediction of the correlation between the process input variables (Concentration of brine, Concentration of binary inhibitor and time) and the output (inhibition efficiency). Mild steel coupons of 20 × 20 × 3 mm size were immersed in 0.5 - 0.9 M of brine, 19–26 mg/ L of binary inhibitor and 8–21 days as designed by RSM to determine the corrosion rate generated by Box Behnken Design Minitab 17 (Tables 1 and 2). Each experimental rum was in triplicate with and without the addition of the binary inhibitor at 27 ^{0}C. At the end of the exposure period, the coupons were cleansed and their weight was noted. The following equation by Satapathy [7] was used to determine the percentage inhibition efficiency (IE%).

$$\textit{Inhibition Efficiency } (IE\,\%) = (M_1 - M_2) \times \frac{100}{M_1} \quad (1)$$

Where M_1 – weight loss of mild steel in uninhibited brine solutions (g); M_2 – weight loss of mild steel in inhibited brine solutions (g).

2.2.1.1. Box-Behnken design. The input process variables were varied into separate levels to note their effect on the corrosion inhibition process. The results obtained from the BBD experimental design matrix was used to derive a mathematical model by applying the RSM quadratic model. The experimental data derived from BBD were used for ANN training using a multilayer normal feed-forward neural network. The design of experiments was built on three variables and four levels as displayed in Table 1, which discussed the actual and coded factors, the total amount of experiments generated by Box-Behnken design was 20. The correlation and interaction between the

Table 1
Experimental range and factors used in Box-Behnken design.

Variables	Coded symbol	Levels and range				
		−2	−1	0	1	2
Concentration Of Brine (M)	Za	0.3	0.5	0.7	0.9	1.1
Concentration of the Binary Inhibitor (mg /L)	Zb	15	19	23	26	30
Time (Days)	Zc	3	8	13	17	21

Table 2
Experimental design of the weight loss experiment on mild steel in binary solution.

Sample No.	Conc. Of Brine (M)	Concentration of the Binary Inhibitor (mg/ L)	Time (Days)	Experimental Inhibition Efficiency (%)	Predicted Inhibition Efficiency (%)		Residual Inhibition Efficiency (%)	
					RSM	ANN	RSM	ANN
1	0.7	23	13	84.00	83.95	84.01	0.05	0.01
2	0.5	26	8	53.00	53.41	52.99	−0.41	0.01
3	0.7	23	13	84.00	83.95	84.01	0.05	0.01
4	0.7	23	3	42.00	41.67	42.00	0.33	0.00
5	0.9	26	8	68.00	68.11	68.03	−0.11	0.03
6	0.9	19	17	79.00	78.83	79.03	0.17	0.03
7	0.7	23	13	84.00	83.95	84.01	0.05	0.01
8	0.9	26	17	77.00	77.38	76.91	−0.38	0.09
9	0.7	30	13	70.00	69.86	70.01	0.14	0.01
10	0.5	19	21	64.00	64.13	64.00	−0.13	0.00
11	0.7	23	13	84.00	83.95	84.01	0.05	0.01
12	0.7	23	13	84.00	83.95	84.01	0.05	0.01
13	1.1	23	17	65.00	64.72	65.04	0.28	0.03
14	0.5	26	17	63.00	62.68	63.01	0.32	0.01
15	0.5	23	8	52.00	52.25	52.01	−0.25	0.01
16	0.7	23	13	84.00	83.95	84.01	0.05	0.01
17	0.9	19	8	68.00	68.51	67.94	−0.51	0.06
18	0.7	15	13	72.00	71.96	72.00	0.04	0.00
19	0.5	19	3	54.00	53.81	54.00	0.19	0.00
20	0.3	23	13	38.00	38.00	38.00	0.00	0.00

variables were determined by fitting the equation of the second-order polynomial to the resulting data obtained. The model quality was evaluated by applying the analysis of variance (ANOVA) and the test of significance. The fitted quadratic response model is given as Eq. (2)

$$Y = d_0 + d_1Y_1 + d_2Y_2 + d_3Y_3 + d_{11}Y_1^2 + d_{22}Y_2^2 + d_{33}Y_3^2 + d_{12}Y_1Y_2 + d_{13}Y_1Y_3 + d_{23}Y_2Y_3 + e \quad (2)$$

Where Y is value predicted for the response (inhibition efficiency), d_0 is the offset term, d_1, d_2, and d_3, are the linear coefficients, d_{11}, d_{22}, and d_{33} are the quadratic coefficients, d_{12}, d_{23}, and d_{23} are cross products and e represents the error term. All the experiments were carried out in triplicates and the mean values were used. The design matric of the BBD experimental sets and the responses observed were tabulated in Table 2. Minitab 17 was used for experimental design and data analysis was performed by BBD response surface design.

2.2.1.2. Artificial neural networks. In the training technique, information was performed in the forward direction from the input layer to the hidden layer, then from the hidden layer to the output layer derived as the assigned network (Fig. 1). The computational application of the ANN program is to conduct simulation as well as prediction. The internal variables and structure can be configured and determined as desired in the designed simulation. In this study, multilayer normal feed-forward neural network training with QuickProp (QP) learning algorithm was developed using Neural Power version 2.5 (CPC-X software, USA). The connection strength between the inputs, hidden and output layers was determined by ANN parameters such as weights and biases.

2.2.2. Linear polarization resistance tests

Linear polarization resistance (LPR) measurements were potentiodynamically executed in ± 10 mV potential range with reference to open circuit potential applied at a scan rate of 0.5 mV/s. The system response (inhibited and uninhibited mild steel in brine solution) was analyzed through Autolab software. Polarization resistance (P) values were obtained from the current corrosion density and equilibrium corrosion potential. From the measured polarization resistance values, the inhibition efficiency (IE%) was determined from the equation:

$$IE\ \%= \frac{P_1 - P_0}{P_0} \times 100 \quad (3)$$

Where P_0 and P_1 are the polarization resistance values with the presence and absence of inhibitors.

2.3. Surface analysis

The morphologies of the mild steel surfaces in inhibited and uninhibited brine solution were analyzed by scanning electron microscope.

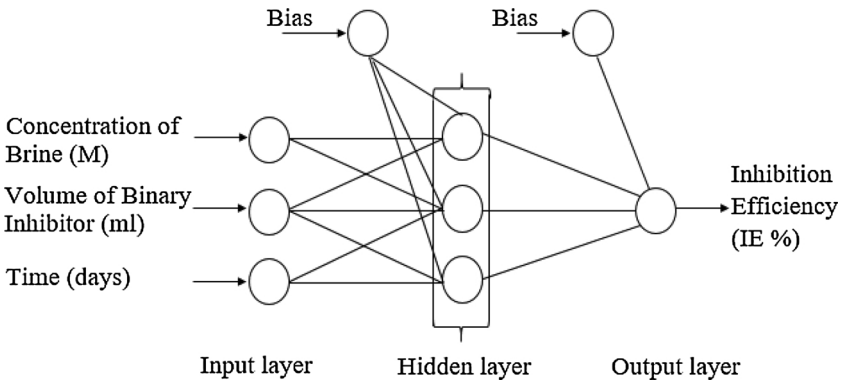

Fig. 1. Structure of ANN architecture for Inhibition efficiency (%) of mild steel.

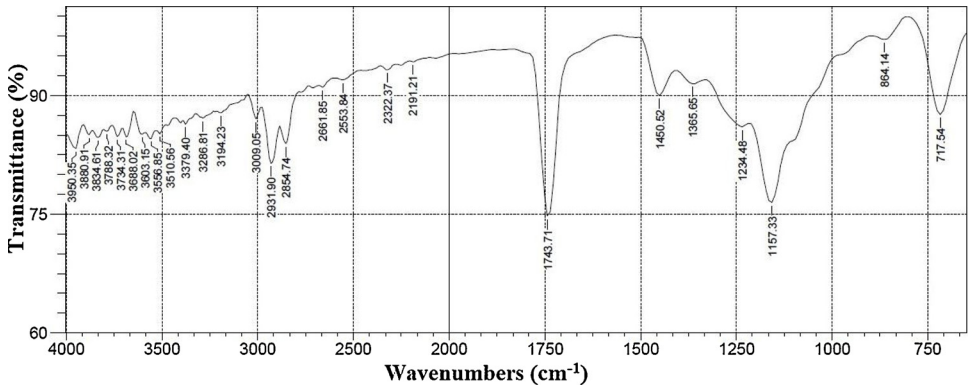

Fig. 2. FT-IR spectra of sesame and castor oil binary inhibitor.

3. Results and discussion

3.1. Results

3.1.1. Characterization of the binary inhibitor

3.1.1.1. FTIR spectrum and results. Fig. 2 illustrates the FT-IR spectrum of the binary mixture of sesame and castor oil. Absorption band observed at 3556.85, 3510.56, 3379.40 and 3286.81 cm^{-1} bands are associated with the broad hydroxyl group. The 3194.23 cm^{-1} bands indicate the presence of ammonium ion in the organic mixture. The peaks at 2931.90 cm^{-1} and 2854.74 cm^{-1} can be assigned to the aliphatic and aromatic stretching mode of C–H groups respectively [7]. The 2553.84 cm^{-1} band is associated with S−H stretching band. The 2191.21 cm^{-1} band can be identified with the CC≡ band. The peak at 1743.71 cm^{-1}corrresponds to the stretching modes of carbonyl groups in organic acids (RCOOH) or ketones (RCOR) and aldehyde (RCOH) or ester (R−−−−−CO-O-R). The peak at 1450.52 $cm^{-1}$is attributed to the methyl C–H asymmetric bend. The peak for phenol or tertiary alcohol bend and aromatic phosphate stretch are noticed at 1365.65 $cm^{-1}$and 1234.48 cm^{-1} respectively. The peak at 1157.33 cm^{-1} implies the stretching mode of C–N. The peaks at 864.14 cm^{-1} and 717.54 cm^{-1} implies the presence of aromatic C–H bend. The occurrence of various bands implies that the binary inhibitor contains a mixture of various compounds like oils, flavonoids, and alkaloids [7,26].

3.1.1.2. GC–MS results. Gas chromatography-mass spectroscopy (GC–MS) spectra of the binary inhibitor used in this study is shown in Fig. 3. It comprise of 7 major peaks as well as many other small peaks indicating the presence of more than 7 major compounds. The small peaks may be associated with compounds present in minute quantities in addition to possible disintegrated major compounds. The 7 major peaks identified are oleic, stearic, methyl ricinoleate, behenic, palmitic, undecylenic, and nonadecyclic acid. The most predominant was oleic acid. Other peaks with low retention time are largely plant compounds with low polarity such as lupenol, friedelin, and b-sitosterol, etc. Unsaturated compounds such as oleic, steric and palmitic acid have been reported for its corrosion inhibitory properties [27], hence, the binary mixture was used to perform corrosion inhibition studies.

3.2. Weight loss measurements

Corrosion inhibition occurs as a result of surface film stabilization on the steel. The effect of chemically stable surface-active inhibitors increases the activation energy of iron dissolution reaction, thus reducing the surface available for corrosion [7]. The increase weight loss with time resulted in a corresponding increase in the inhibition efficiency [28] in the presence and absence of binary inhibitor. This indicates that insoluble surface film was not created on the electrode surface during mild steel corrosion in brine solutions [13]. It implies that the binary inhibitor was first adsorbed on the surface of the electrode impeding corrosion either by blocking the reaction sites or by altering the mechanism of anodic and cathodic corrosion process [28]. Therefore, the inhibitive nature of binary mixture in brine solutions results from electrostatic adsorption of a negatively charged

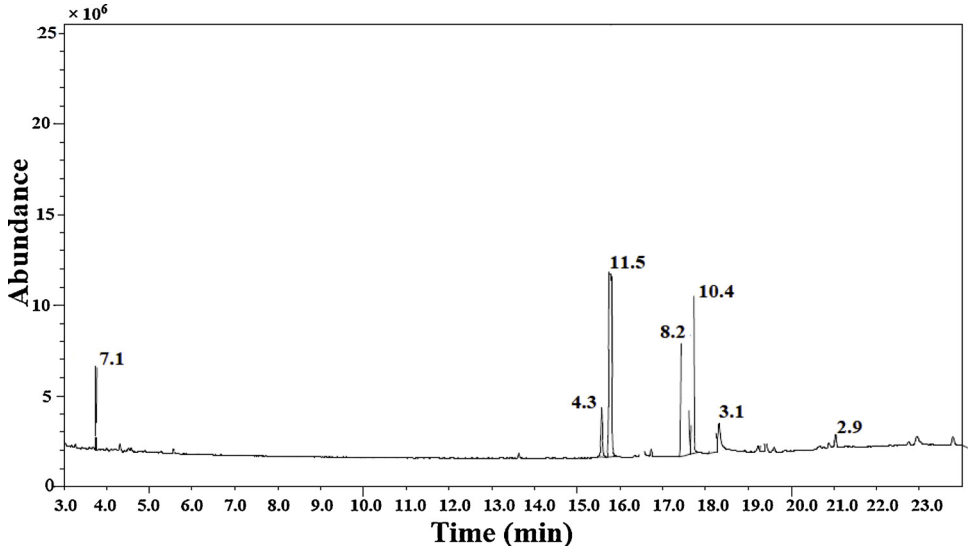

Fig. 3. GC–MS of sesame and castor oil binary inhibitor.

deprotonated mixture of the binary inhibitor to the positively charged electrode surface, thus forming a barrier on the steel surface. The surface film protects the mild steel against corrosive ions, such as Cl^- of OH^- [13].

The design matrix obtained from the Box Behnken response surface optimization tool is used to derive a quadratic model that emphasizes the effect of interactional and individual effect of process variables and their level of significance in the process. The design matrix obtained from the Box Behnken design was utilized for the ANN training.

3.2.1. Molding using Box Behnken design – response surface methodology

From the experimental results, an empirical relationship between the response (Inhibition Efficiency) and independent variable (Concentration of brine, Concentration of binary inhibitor and time) in coded terms is expressed in the equation below.

$$\begin{aligned} \textit{Inhibition Efficiency}(\%) = {} & -226.27 + 310.17\,Za + 10.610\,Zb + 10.205\,Zc \\ & - 195.30\,Za^2 - 0.23409\,Zb^2 - 0.34971\,Zc^2 \\ & - 0.01664\,Zb\,Zc \end{aligned} \quad (4)$$

Where Za represents the concentration of brine, Zb represents the concentration of Binary inhibitor and Zc represents immersion time.

The predicted response values (Inhibition efficiency %) have been determined by using the quadratic model in Eq. (4) and are given in Table 2. From the results presented in Table 2, it can be affirmed that there is a good agreement between the experimental values and Box-Behnken RSM predicted values, therefore validating the accuracy of the proposed model. The analysis of variance (ANOVA) results were summarized by the quadratic model demonstrate the adequacy and significance of the model, presented in Table 3.

According to Table 3, the F-value of the model (6609.52) indicates that the model is statistically significant [29–31]. The co-efficient of determination (R^2) was determined to be 99.97%, which implies that more than 99% of the experimental data were compatible and only about 0.03% of the total variation cannot be described by the model. High R^2 value implies that the test variations of 99.97% could be fitted by the model Eq. (4). Adjusted R^2 is used to calculate the model adequacy, the fitness of the model as well as to rectify the R^2 value for sample size and for the set of terms in the model. A high value of adjusted R^2 (99.96%) implies a high model significance.

The optimum condition of independent variables selected for the best inhibition efficiency (%) of the model as predicted statistically by Minitab 17 software was corrosion inhibition of 86.2% at variable conditions of 0.79 M concentration of brine, 22.1 mg/ L concentration of binary inhibitor and at a time period of 14 days.

3.2.2. ANN modelling

Several neural network architectures, topologies, and transfer functions have been identified and analyzed for prediction of inhibition efficiency of a binary mixture of sesame and castor oil in brine solution (%). The selection of suitable network architecture, its transfer function, and its topology is essential for the successful application of ANN as a type of transfer function used to control the learning rate of a neural network and its performance. The number of neurons was incited by a heuristic approach involving testing different amounts of neurons and topology until the mean square error (MSE) of the output data was reduced by varying the topology (4:n:3) and the number of neurons (n) used from 7 to 21.

ANN architecture was trained using 1000 as a stopping criterion. The mean square error (MSE) and the coefficient of determination were evaluated to determine the neural network predictive ability. The mean square error (MSE) and the coefficient of determination were calculated using the equations below.

$$R^2 = 1 - \sum_{j=1}^{n} \left(\frac{(z_{j,cal} - z_{j,exp})^2}{(z_{avg,exp} - z_{j,exp})^2} \right) \quad (5)$$

$$MSE = \frac{1}{n} \sum_{j=1}^{n} (N_j - Z_j)^2 \quad (6)$$

Where, $z_{j,cal}$ is the calculated values, $z_{j,exp}$ is the experimental values, $z_{avg,exp}$ is the average experimental values, Nj is the predicted values, Zj is the experimental value, n is the number of runs performed in the experiment. MSE value was established as 0.072984 and the coefficient of determination (R^2) was 0.99999. The predicted values by ANN was in good accordance with the experimental values. The coefficient of determination (R^2) for inhibition efficiency is 0.99998. The weights and bias for the output and hidden layer are illustrated in Table 4.

3.2.3. Experimental analysis of results

3D response surface and contour plots (Figs. 4–6) are the graphical illustration of the quadratic equations to demonstrate the effect of variables on the responses. From Fig. 4, it can be observed that at low concentration of binary inhibitor and low concentration of brine the inhibition efficiency achieved was highest. Increasing the concentration of brine at low concentration of binary inhibitor decreases the inhibition efficiency, these could be attributed to high concentration brine providing a more corrosive environment for the mild steel and less concentration of inhibitor is available to slow down the rate of the corrosion process. A high concentration of inhibitor of 23 mg/ L in a brine concentration of 1.1 M provides inhibition efficiency of 65% compared to the same concentration of inhibitor of 23 mg/ L in a lower brine concentration of 0.7 M with 84% inhibition efficiency. This can be attributed to the fact that a higher concentration of brine has a more corroding effect than a lower brine concentration. Fig. 5 adduced that at a low reaction time and low concentration of brine the inhibition efficiency was at maximum. Increasing the concentration of brine at

Table 3
ANOVA table for inhibition efficiency of the binary inhibitor.

Source	Sum of squares	DF	Contribution (%)	Adj SS	Adj MS	F-Value	P-Value
Model	4055.90	7	99.97	4055.90	579.41	6609.52	0.000
Za	973.42	1	23.99	913.76	913.76	10423.45	0.000
Zb	1.68	1	0.04	3.03	3.03	34.55	0.000
Zc	280.96	1	6.93	666.68	666.68	7604.98	0.000
Za^2	1465.69	1	36.13	1461.85	1461.85	16675.73	0.000
Zb^2	80.84	1	1.99	261.66	261.66	2984.80	0.000
Zc^2	1252.75	1	30.88	1253.27	1253.27	14296.37	0.000
Zb × Zc	0.56	1	0.01	0.56	0.56	6.37	0.027
Error	1.05	12	0.03	1.05	0.09		
Lack-of-Fit	1.05	7	0.03	1.05	0.15		
Pure Error	0.00	5	0.00	0.00	0.00		
Total	4056.95	19	100.00				

R2 = 99.97%, Adjusted R^2 = 99.96%, Predicted R^2 = 99.88%.
Where DF = Degree of freedom, Adj SS = Adjusted sum of squares, Adj MS = Adjusted Mean squares.

Table 4
Weights for hidden and output layer.

Layer	Weights of the hidden layer			Output (% IE)
	1	2	3	
Neuron 1	9.7402	9.7457	2.0950	1.4829
Neuron 2	−5.2592	6.3340	0.1662	1.0844
Neuron 3	−3.8168	2.8469	−0.5160	−5.8163
Bias	−2.4523	11.4532	0.1376	−3.3066

low reaction time reduces the inhibition efficiency, this can be as a result of a more corrosive environment provided by a higher concentration of brine. Although, as time increases and the concentration of brine reduces the inhibition efficiency is at maximum. This can be attributed to a reduction in the concentration of brine resulting in a less corrosive environment for the mild steel. From Fig. 6, it can be observed that at low reaction time and low concentration of binary inhibitor the inhibition efficiency reduces, and as the time increases and the concentration of inhibitor increases the inhibition efficiency increases. For instance, increasing the concentration of inhibitor from 23 to 30 mg/ L at a constant period of time 3 days, the inhibition efficiency increases by 32%. This further proves the efficiency of the binary inhibitor in inhibiting the corrosion rate of mild steel in brine solutions.

The relative significance of the three input variables was evaluated using Neural Power version 2.5 (CPC-X software, USA) shown in Fig. 7. As displayed in Fig. 7, all of the three variables (Concentration of brine, Concentration of binary inhibitor, and Time with a relative importance of 53.26%, 29.02%, and 17.72% respectively) have strong effects on the inhibition efficiency. Therefore, all the variations studied in this work could not be negated in this current analysis. The degree of potency of variables was found in the following order of

Concentration of brine > Concentration of binary inhibitor > Time

3.2.4. Comparison of ANN and RSM models

The predictive execution of the ANN and RSM models were compared on the basis of coefficient of determination (R^2), Relative Percent Deviation (RPD) and Root Mean Square Error (RMSE) given by the model. The general model capability can be validated in the prediction accuracy for the authentication of a data set. The values of R^2, RPD, and RMSE for the ANN model were greater than those for the RSM model as shown in Table 5. This result implies that the ANN model for prediction has higher accuracy than the RSM model used for prediction. This also indicates that the experimental data has a high level of accuracy fitted using the ANN model.

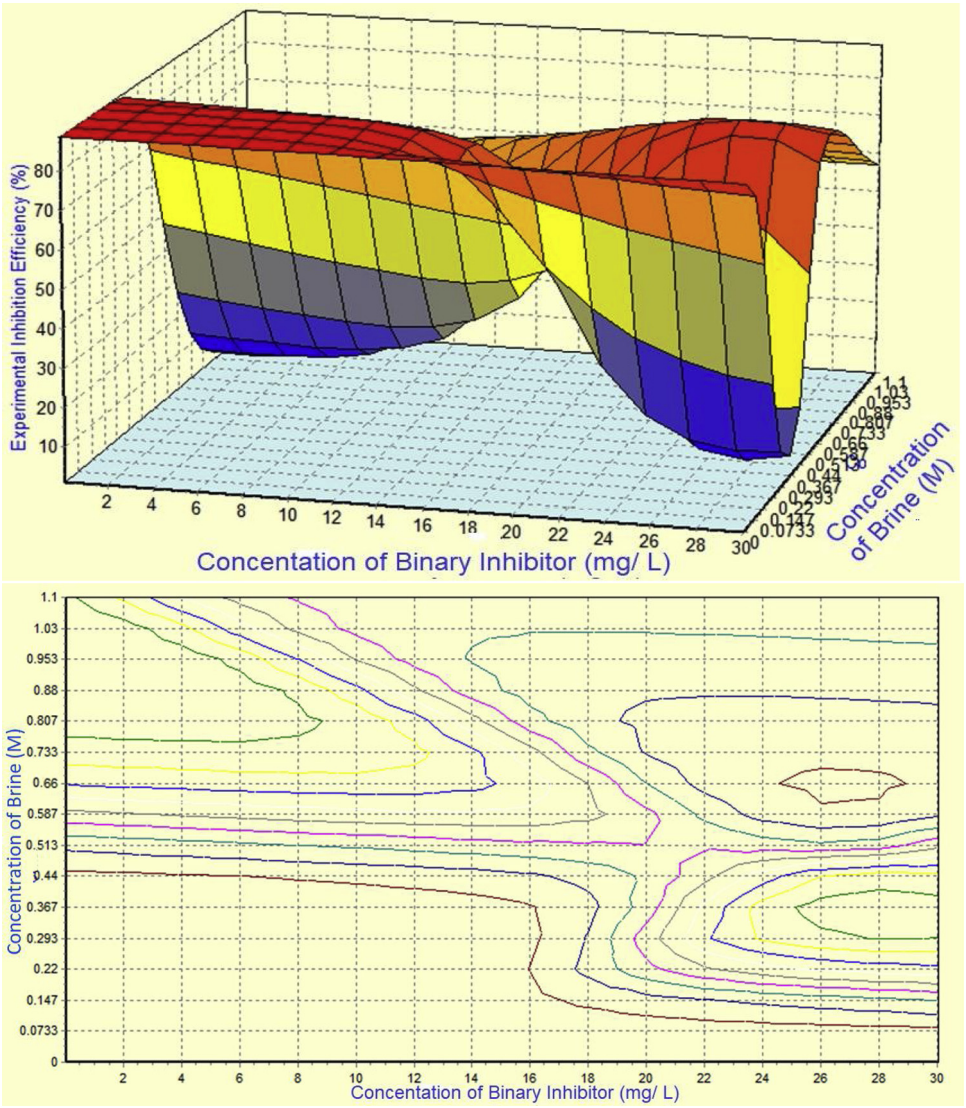

Fig. 4. Surface and contour plots illustrating the effects of brine concentration (M) and Concentration of binary inhibitor (mg/ L) on Inhibition efficiency (%).

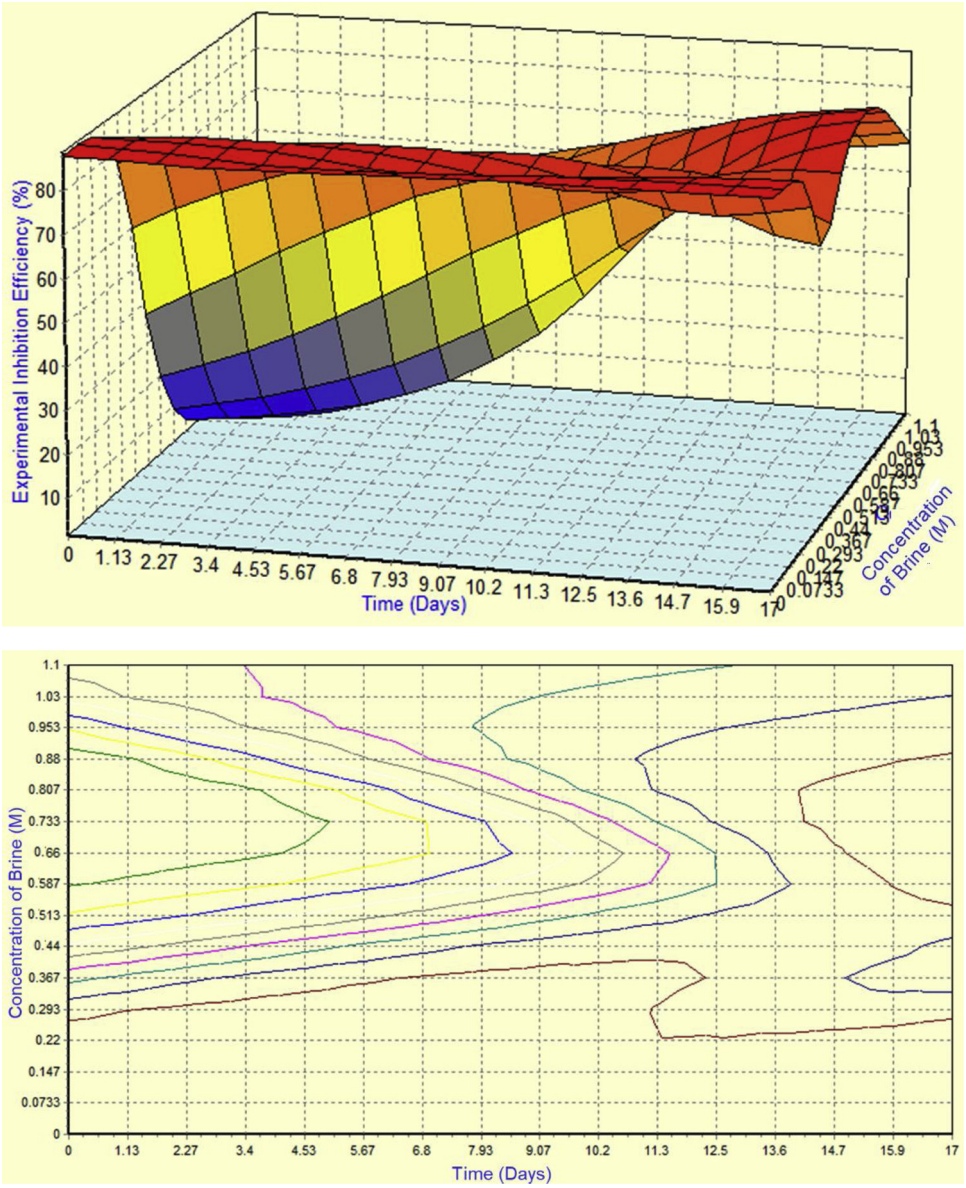

Fig. 5. Surface and contour plots illustrating the effects of brine concentration (M) and Time (days) on Inhibition efficiency (%).

In the validation of the experimental data set, R^2, RPD and RMSE values for the RSM and ANN models are displayed in Table 5. Table 5 showed that both models gave a very high performance of the data set validation, but ANN performed invariably better than RSM. The performance prediction of the ANN model for data set validation affirms a greater capacity for the generalization on the given case over RSM. Also, Fig. 8 illustrates the predicted and experimental values for each experimental run to obtain the inhibition efficiency. From Fig. 8, it is obvious that the trained neural network has an effective approximated experimental values. The higher predictive capability of the ANN can be ascribed to its potential to generally approximate the system nonlinearity, in contrast to RSM which is limited to second-order degree polynomial [29]. Nevertheless, when the ANN technique is used it must be noted that its predictions are limited to the range of process factors applied in the training process [29,32]

3.3. Effect of immersion time

The variation of inhibition efficiency with immersion time is illustrated in Figs. 5 and 6. Fig. 5 illustrates the changes observed in the experimental inhibition efficiency against immersion time and concentration of brine. At low brine concentration, the inhibition efficiency increases with time this was in agreement with previous studies [33,34]. Also, at a high concentration of brine, the inhibition efficiency increases as time increases. A similar occurrence was also experienced in Fig. 6. The inhibition efficiency increases as the immersion time was increased at a low concentration of binary inhibitor. Similarly, increasing the concentration of binary inhibitor to maximum, the inhibition efficiency increased as the immersion time increased but after 10 days of immersion the inhibition efficiency decreases indicating that the inhibition potential of inhibitors decreased as a function of their exposure in acid [35]. Overall, for this study, the relative importance of immersion time is 17.72% which was lower than the concentration of brine and concentration of binary inhibitor of 53.26% and 29.02% respectively (Fig. 7).

3.4. Potentiodynamic polarization

The effects of a binary mixture of sesame and castor oil on the behavior of anodic and cathodic polarization of mild steel in brine

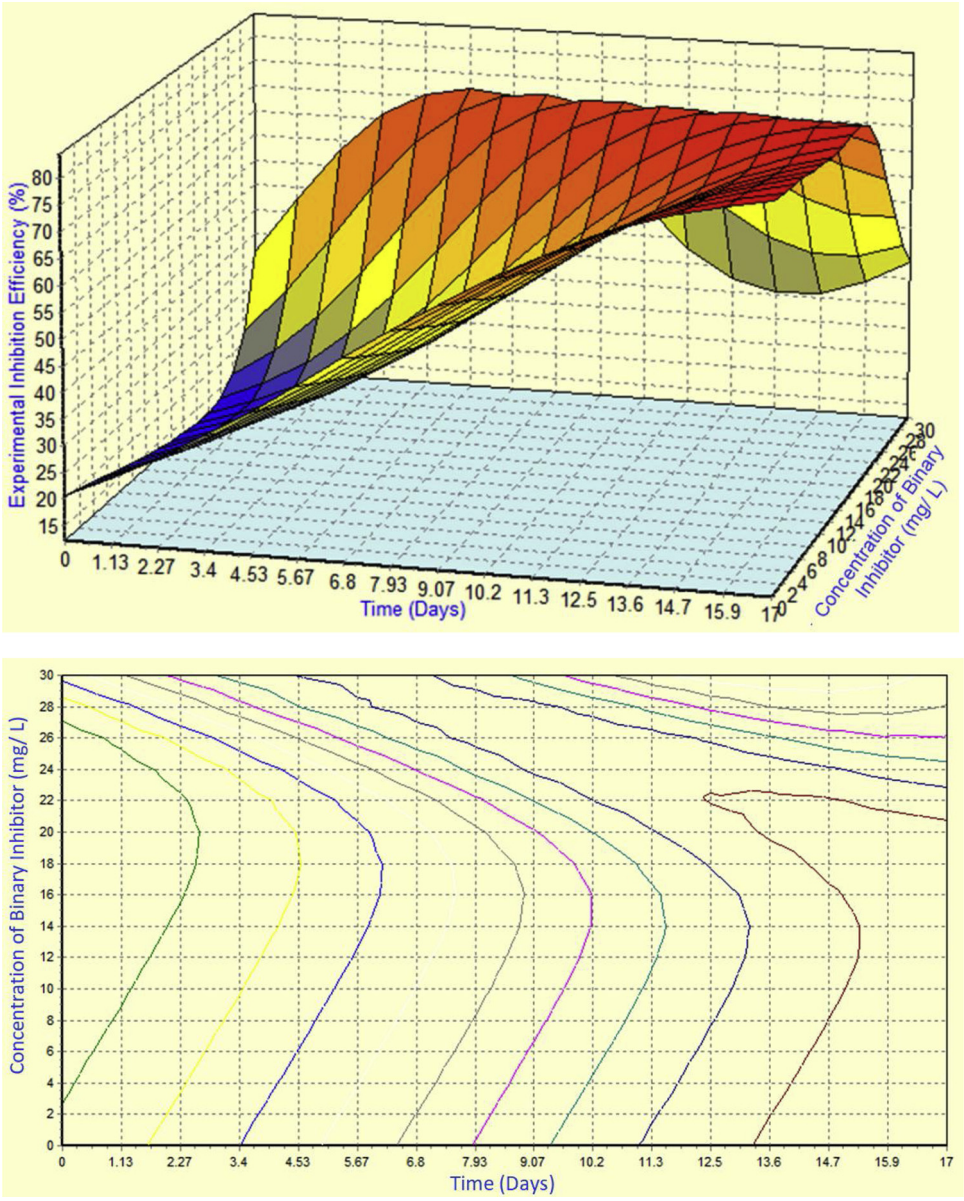

Fig. 6. Surface and contour plots illustrating the effects of Concentration of Binary inhibitor (mg/ L) on Time (Days).

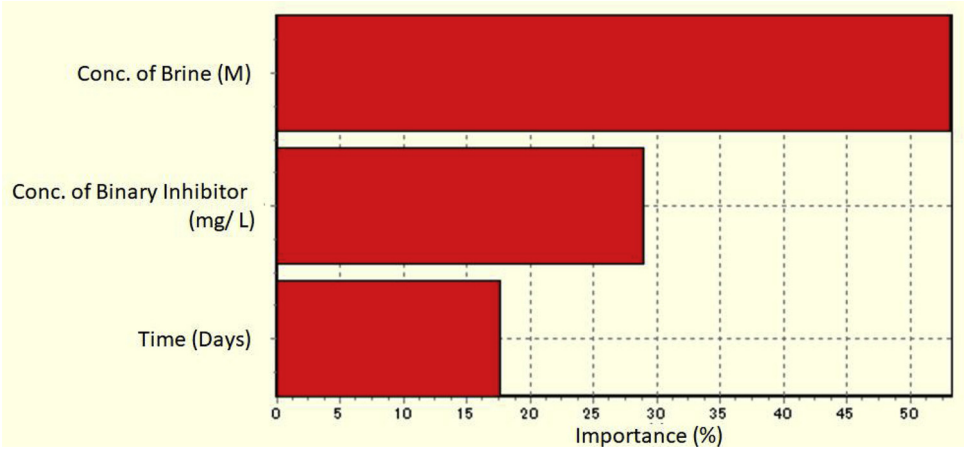

Fig. 7. Relative importance of the variables on the response.

Table 5
Validation data for RSM and ANN model developed using R^2, RPD and RMSE.

Factors	Models	
	RSM	ANN
Coefficient of determination (R^2)	0.99970	0.999990
Relative percent deviation (RPD)	5.03568	5.383000
Root mean square error (RMSE)	0.29608	0.072984

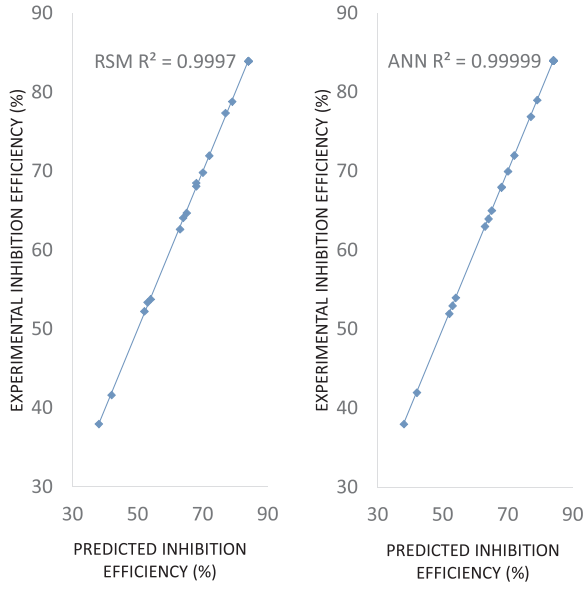

Fig. 8. Comparing experimental and predicted values for RSM (left) and ANN (right).

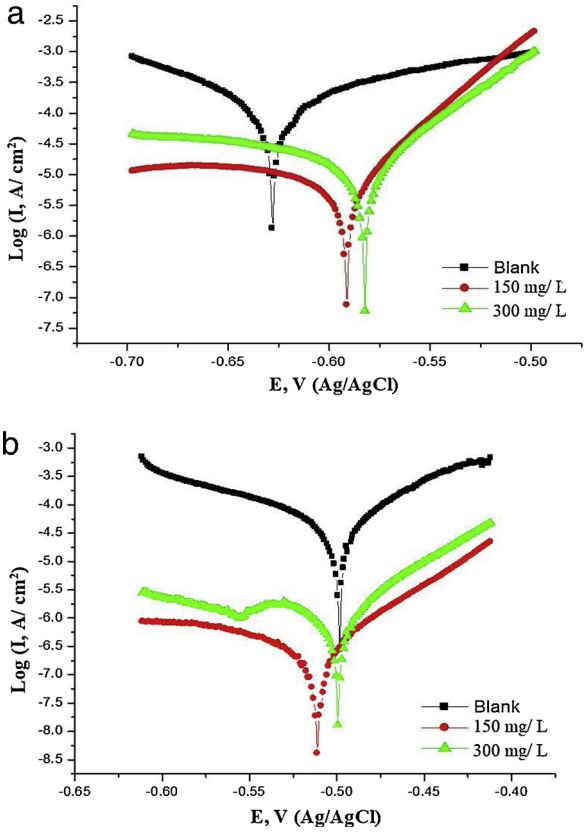

Fig. 9. a. The log of current against potential for 0.3 M Brine. b. The log of current against potential for 1.1 M Brine.

solution have been investigated by polarization measurements and recorded as displayed on the Tafel plots in Fig. 9a and b for 0.3 M and 1.1 M concentration of brine respectively. It is illustrated from the data presented in Table 6 that both cathodic hydrogen evolution and anodic metal dissolution of mild steel reaction were inhibited with the addition of the binary mixture of sesame and castor oil to 0.3 M and 1.1 M of brine solution. The inhibitory nature of this reaction was more visible with the further addition of the binary inhibitor.

Fig. 9a and b illustrate the effect of the binary inhibitor (equal volumes of sesame and castor oils) on the kinetics of mild steel corrosion inhibition process in 0.3 and 1.3 M of brine solutions. Inhibitor added in brine solutions influence the corrosion reactions and could be observed by the changes in the corrosion potentials as well as alterations in both cathodic and anodic polarization curves. The equilibrium corrosion potentials (E_{pcorr}) is altered towards more negative values in the presence of inhibitor. Also, decreasing the cathodic polarization curves was above the anodic polarization curves. Both observations imply that the inhibitor reduces the cathodic corrosion reactions successfully than anodic corrosion reaction [36]. Further analysis showed that the polarization curves were slightly altered when different amounts of inhibitor were added in 0.3 M brine solution (Fig. 9a). This reveals that the amount of inhibitor added has little effect on the inhibition mechanism.

The technical terms associated with the kinetics of corrosion process, such as, equilibrium corrosion potential (E_{pcorr}), corrosion current density (I_{pcorr}), anodic Tafel slope (b_c) and cathodic Tafel curve slope (b_a) was calculated from the polarization curves at different inhibitor concentrations and an over-view was stated in Table 2. Observing the values of E_{pcorr} showed that the addition of more of the binary inhibitor caused the corrosion potential of the mild steel to shift towards a greater negative potential with reference to E_{pcorr} in 0.3 and 1.1 M of brine solutions. According to Riggs and others [37], a compound is classified as anodic or cathodic inhibitor based on the displacement of E_{pcorr}, if the displacement is > 85 mV in reference to E_{pcorr} the inhibitor can be reported as a cathodic or anodic inhibitor, otherwise, it will be classified as a mixed type inhibitor. In this study, the maximum change observed in the corrosion potentials was 60.42 mV and 117.81 mV in 0.3 M and 1.1 M brine solution respectively. The binary inhibitor used in this study can be classified as a mixed corrosion inhibitor in moderately low concentration range for brine solutions this was corroborated by Popoola [22] for sesame oils. Thus, this type of binary inhibitor simultaneously acts as anodic and cathodic inhibitors in a higher concentration of brine solutions. The values of anodic and cathodic (b_a and b_c) slopes presented in Table 6 were changed significantly as the concentration of inhibitor, this suggests that inhibitor adsorption on the metal surface probably affects the mechanism at which mild steel dissolves in brine solutions.

Table 6 illustrate that further addition of inhibitor reduces the corrosion current in concordance with the concentration of inhibitor used. The values of corrosion current density were obtained by extrapolation of cathodic Tafel (b_c) lines to the respective free corrosion potential (E_{corr}) [22]. The lowest I_{pcorr} value was deduced for both concentrations (0.3 and 1.1 M brine) at 300 mg /L concentration of binary inhibitor. However, using 0.3 M of brine the corrosion current value was lower than in 1.1 M of brine, showing the binary mixture was more effective corrosion inhibitor in 0.3 M of brine solution than 1.1 M brine solution. The basis for mild steel corrosion inhibition of mild steel in brine solutions can be as a result of the resistance values of linear polarization (R_p). The resistance of the mild steel polarization in brine solutions was significantly increased in the presence of the inhibitor (Table 6). Consequently, corrosion inhibition was realized. On the other hand, it can be declared that the adsorption of inhibitor molecules on the mild steel surface at the active cathodic and anodic sites made the

Table 6
Kinetic parameters obtained from Tafel plots of mild steel immersed in 0.3 M and 1.1 M Brine containing the binary inhibitor.

Brine Solution	Conc of Binary inhibitor (mg/ L)	E_{pcorr} (mV vs Ag/AgCl)	I_{pcorr} (μA/cm^2)	b_a (mV/ dec)	b_c (mV/ dec)	Rp (Ω cm^2)	IE %
0.3 M NaCl	Blank	495.22	1610	390.6	28.40	44.49	–
	150	480.08	708	15.96	34.25	668.04	99.56
	300	434.8	293	31.64	12.27	1311.3	98.18
1.1 M NaCl	Blank	628.83	4100	49.03	16.87	13.28	–
	150	512.97	411	31.96	15.89	112.15	89.99
	300	511.07	348	50.47	9.08	959.26	91.52

metal (mild steel) more protected from corrosion (polarization) resulting into corrosion inhibition.

It can be summarized that the binary inhibitor (sesame and castor oil) preferentially adsorbed on the active sites of the mild steel surface resisting corrosion reaction by improving the electrode insulation potential (low corrosion current). Inhibitor concentration improves the inhibition efficiency accompanied by a low change in corrosive solutions. Larger surface coverage and low rate of adsorption of inhibitor molecules can be adjured by the stated fact.

3.5. Electrochemical impedance spectroscopy (EIS)

Electrochemical impedance spectroscopy was used to obtain more information about the kinetics of mild steel corrosion in the presence of the binary inhibitor mixture (sesame and castor oil). The electrochemical process takes place at the open-circuit potential and was examined by the electrochemical impedance spectroscopy. EIS measurements of the mild steel electrode at its open circuit potential were observed after immersing in brine solution alone for 15 min and in the presence of different concentrations of the binary mixture. These experiments were performed over a 10 kHz to 10 mHz frequency range. Fig. 10 illustrates the Nyquist plots for mild steel dissolution in uninhibited and inhibited brine solution with different concentrations of the binary inhibitor. It was observed that the width of the Nyquist plots increased as the concentration of the binary inhibitor increased, indicating the strengthening of the inhibitive film. Furthermore, the Nyquist plots present imperfect semicircle which occurs due to the rough electrode surface and surface homogeneity [38]. The EIS spectrum recorded for mild steel in 1 M brine solution at 27 ^{0}C (Fig. 10) showed one depressed capacitive loop. This same trend was also observed in mild steel immersed in 1 M brine containing binary inhibitor (15–30 mg/L). The depressed semicircle with the center under the real axis is a characteristic behavior of a solid electrode attributed to the roughness of the surface and inhomogeneity of the metal electrodes [7].

EIS experiment was performed for mild steel immersed in 1 M Brine solution uninhibited and inhibited with binary inhibitor at 27 ^{0}C as shown in Fig. 10. The respective kinetic parameters are displayed in

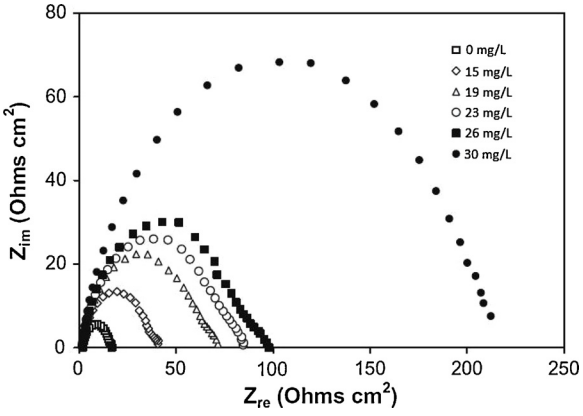

Fig. 10. Nyquist plot for mild steel in 1 M brine uninhibited and inhibited with different concentration of the binary inhibitor.

Table 7
EIS parameters obtained for mild steel in 1 M Brine uninhibited and inhibited with binary inhibitor.

Inhibitor	Conc (mg/L)	Rs (Ω cm^2)	R_{ct} (Ω cm^2)	C_{dl} (μF cm^{-2})	IE
Blank	–	0.92	11.34	103.63	0.78
Binary inhibitor	15	0.906	34.72	78.91	0.79
	19	0.926	63.54	64.79	0.81
	23	0.917	72.78	65.77	0.82
	26	0.907	94.67	63.98	0.84
	30	1.053	207.62	59.47	0.86

Where Rs is the solution resistance, R_{ct} is the charge transfer resistance and C_{dl} is the double layer capacitance.

Table 7. The EIS plots of mild steel in brine solution uninhibited and inhibited with the binary inhibitor at 27 ^{0}C showed an inductive loop in low frequency (LF) region while it displays a depressing capacitive loop at high-frequency region (HF). Thus indicates the occurrence of a Faradaic process on free electrode sites. From EIS illustrated in Table 7, the charge transfer resistance (R_{ct}) values increases as the concentration of binary inhibitor increase, thus indicating the formation intermediates responsible for the anodic controlling process from the metal dissolution and subsequently inhibiting corrosion. It was also observed that the R_{ct} values increase whereas the double-layer capacitance (C_{dl}) values decrease in the presence of the binary inhibitor at different concentrations. The increase in the R_{ct} and decrease in C_{dl} values in inhibited solutions are due to a reduction in local dielectric constant and/or to an increase in the thickness of the double layer [39]. These results imply that the binary inhibitor in this study inhibits mild steel corrosion by adsorbing on the metal/electrode interface [38]. The adsorption of the binary inhibitor on the electrode reduces the electrical capacity because it displaces water molecules and other ions initially adsorbed on the surface. The depletion of this capacity with increasing binary inhibitor concentration may be due to the formation of a protective layer at the surface [7]. The maximum value of R_{ct} attained was 207.62 Ω cm^2 for binary inhibitor at 27 ^{0}C. The results obtained in this study showed that the binary mixture of sesame and castor oil acts as a good corrosion inhibitor at 27 ^{0}C in brine solutions.

3.6. Surface characterization

To ascertain whether corrosion inhibition occurs as a result of the formation of a protective film by the binary inhibitor on the metal surface, SEM images were taken. Fig. 11 illustrates the surface morphology of the SEM analysis of the examined samples. The figure shows the micrograph of mild steel examined after exposure to 0.5 and 1.1 M of brine solution. The figures reveal the SEM images after immersion, severe damage on the surface occurs as a result of material dissolution starting on grain boundaries located between perlite and ferrite. Grain boundaries are well known to be active sites where lattice and dislocation defects accumulate, therefore the deposition of iron oxide/oxyhydroxide is often initiated on the grain boundaries to be slowly spread evenly on the whole metal surface. The rate at which mild steel degrades depends on the presence of a good protective film on its surface.

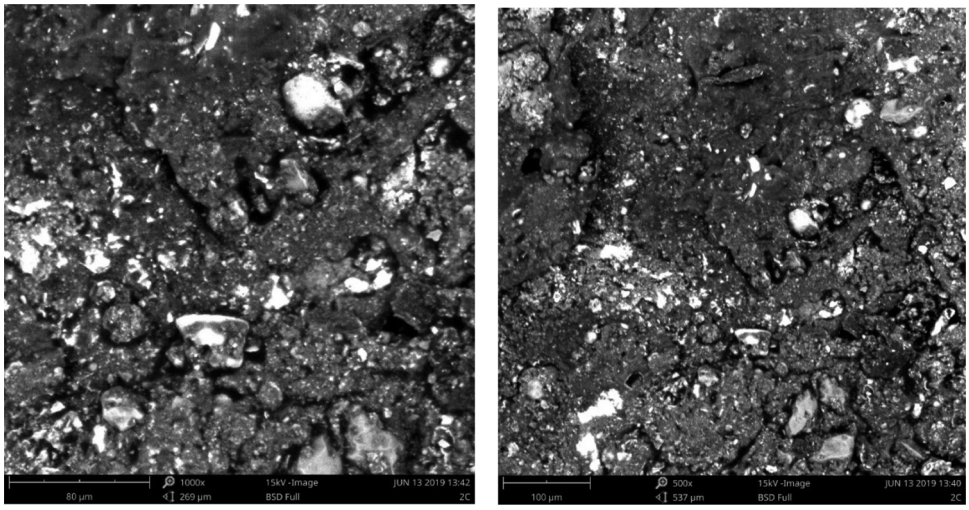

Fig. 11. SEM images of corroded mild steel in brine solution.

4. Conclusion

The results presented in this study (weight loss tests, polarization tests, and SEM micrography) demonstrates the use of a binary mixture of sesame and castor oil as a good corrosion inhibitor. Using Minitab statistical software to determine the weight loss measurements, optimum condition of the independent variable selected by the software for best inhibition efficiency was corrosion inhibition of 86.2% at 0.79 M brine concentration, 22.1 mg/ L concentration of binary inhibitor and at a time period of 14 days. The polarization studies demonstrate that binary mixture of sesame and castor oil act as a mixed type inhibitor in moderately low concentration of brine solutions while at high brine concentration it simultaneously acts as anodic and cathodic inhibitors. The study suggests that adsorption of inhibitors on the metal surface probably affects the mechanism at which mild steel dissolves in brine solutions.

Declaration of Competing Interest

The authors declare that they have no known competing financial interests or personal relationships that could have appeared to influence the work reported in this paper.

References

[1] R. Gharibi, M. Yousefi, H. Yeganeh, Synthesis, characterization and assessment of poly (urethane-co-pyrrole)s derived from castor oil as anticorrosion coatings for stainless steel, Prog. Org. Coat. 76 (10) (2013) 1454–1464.
[2] C. Verma, E.E. Ebenso, M.A. Quraishi, Ionic liquids as green and sustainable corrosion inhibitors for metals and alloys: an overview, J. Mol. Liq. 233 (2017) 403–414.
[3] S. Masadeh, The effect of added carbon black to concrete mix on corrosion of steel in concrete, J. Miner. Mater. Charact. Eng. 3 (2015) 271–276.
[4] E.W. Brooman, Modifying organic coatings to provide corrosion resistance. Part II. Inorganic additives and inhibitors, Met. Finish. 100 (2002) 104–110.
[5] V. Sauvant-Moynot, S. Gonzalez, J. Kittel, Self-healing coatings: an alternative route for anticorrosion protection, Prog. Org. Coat. 63 (2008) 307–315.
[6] P.R. Roberge, Corrosion inhibitors, Handbook of Corrosion Engineering, McGraw-Hill, New York, 1999.
[7] A.K. Satapathy, G. Gunasekaran, S.C. Sahoo, K. Amit, P.V. Rodrigues, Corrosion inhibition by Justicia gendarussa plant extract in hydrochloric acid solution, Corros. Sci. 51 (2009) 2848–2856.
[8] E.E. Oguzie, Studies on the inhibitive effect of Occimum viridis extract on the acid corrosion of mild steel, Mater. Chem. Phys. 99 (2006) 441.
[9] P.C. Okafor, M.E. Ikpi, I.E. Uwah, E.E. Ebenso, U.J. Ekpe, S.A. Umoren, Inhibitory action of Phyllanthus amarus extracts on the corrosion of mild steel in acidic media, Corros. Sci. 50 (2008) 2310.
[10] I. Radojcic, K. Berkovic, S. Kovac, J.V. Furac, Natural honey and black radish juice as tin corrosion inhibitors, Corros. Sci. 50 (2008) 1498.
[11] P.B. Raja, M.G. Sethuraman, Natural products as corrosion inhibitor for metals in corrosive media – a review, Mater. Lett. 62 (2008) 113.
[12] E.E. Oguzie, Evaluation of the inhibitive effect of some plant extracts on the acid corrosion of mild steel, Corros. Sci. 50 (2008) 2993.
[13] M.A. Amin, S.S.A. El-Rehim, E.E.F. El-Sherbini, R.S. Bayoumy, The inhibition of low carbon steel corrosion in hydrochloric acid solutions by succinic acid: part I. Weight loss, polarization, EIS, PZC, EDX and SEM studies, Electrochim. Acta 52 (2007) 3588.
[14] R.S. Gonçalves, L.D. Mello, Electrochemical investigation of ascorbic acid adsorption on low-carbon steel in 0.50 M Na2SO4 solutions, Corros. Sci. 43 (2001) 457.
[15] D.Q. Zhang, Q.R. Cai, L.X. Gao, K.Y. Lee, Effect of serine, threonine and glutamic acid on the corrosion of copper in aerated hydrochloric acid, Corros. Sci. 50 (2008) 3615.
[16] A. Bouyanzer, B. Hammouti, L. Majidi, Pennyroyal oil from Mentha pulegium as corrosion inhibitor for steel in 1 M HCl, Mater. Lett. 60 (2006) 2840.
[17] F.S. de Souz, A.A. Spinelli, Caffeic acid as a green corrosion inhibitor for mild steel, Corros. Sci. 52 (2009) 1845.
[18] S. Godavarthi, J. Porcayo-Calderon, M. Casales-Diaz, E. Vazquez-Velez, A. Neri, L. Martinez-Gomez, Electrochemical analysis and quantum chemistry of castor oil-based corrosion inhibitors, Curr. Anal. Chem. 12 (5) (2016) 476–488.
[19] M. Omotioma, O.D. Onukwuli, Corrosion inhibition of mild steel in 1.0 m HCl with castor oil extract as inhibitor, Int. J. Chem. Sci. 14 (1) (2016) 103–127.
[20] J.A. Udiandeye, A.O. Okewale, B.R. Etuk, P. Igbokwe, Investigation of the use of ethyl esters of castor seed oil and rubber seed oil as corrosion inhibitors, Int. J. Basic Appl. Sci. 11 (6) (2011) 48–54.
[21] M. Abdallah, I. Zaafarany, K.S. Khairou, Y. Emad, Natural oils as corrosion inhibitors for stainless steel, Chem. Technol. Fuels Oils 48 (3) (2012) 46–52.
[22] A.P.I. Popoola, M. Abdulwahab, O.S.I. Fayomi, Corrosion inhibition of mild steel in Sesamum indicum - 2M HCl / H2SO4 interface, Int. J. Electrochem. Sci. 7 (2012) 5805–5816.
[23] B.V. Ayodele, C.K. Cheng, Modeling and optimization of syngas production from methane dry reforming over ceria supported cobalt catalyst using artificial neural networks and Box-Behnken design, J. Ind. Eng. Chem. 32 (2015) 246–258.
[24] E. Betiku, A.E. Taiwo, Modeling and optimization of bioethanol production from breadfruit starch hydrolyzate vis-à-vis response surface methodology and artificial neural network, Renew. Energy 74 (2015) 87–94.
[25] A.M. Yadav, S. Nikkam, P. Gajbhiye, M.H. Tyeb, Modeling and optimization of coal oil agglomeration using response surface methodology and artificial neural network approaches, Int. J. Miner. Process. 163 (2017) 55–63.
[26] K. Mruthunjaya, V.I. Hukkeri, Antioxidant and free radical scavenging potential of Justicia gendarussa Burm leaves in vitro, Nat. Prod. Sci. 13 (2007) 199.
[27] A. Khanra, M. Srivastava, M.P. Rai, R. Prakash, Application of unsaturated fatty acid molecules derived from microalgae toward mild steel corrosion inhibition in HCl solution : a novel approach for metal − inhibitor association, ACS Omega 3 (2018) 12369–12382.
[28] M. Abdallah, E.A. Helal, A.S. Fouda, Aminopyrimidine derivatives as inhibitors for corrosion of 1018 carbon steel in nitric acid solution, Corros. Sci. 48 (7) (2006) 1639–1654.
[29] A. Sarve, S.S. Sonawane, M.N. Varma, Ultrasound assisted biodiesel production from sesame (Sesamum indicum L.) oil using barium hydroxide as a heterogeneous catalyst: comparative assessment of prediction abilities between response surface methodology (RSM) and artificial neural network (ANN), Ultrason. Sonochem. 26 (2015) 218–228.
[30] D.T. Oyekunle, D.O. Oyekunle, Biodiesel production from yellow oleander seed oil via heterogeneous catalyst: performance evaluation of minitab response surface methodology and artificial neural network, J. Mater. Environ. Sci. 9 (8) (2018) 2468–2477.
[31] T. Oguntade, O. Rotimi, A. Mojisole, A. Solomon, G. Angye, Experimental dataset of enhanced rheological properties and lubricity of Nigerian bentonite mud using kelzan® xcd polymer and identifying it optimal combination, Data Brief (2018) 1804–1809.

[32] K.M. Rajkovic, J.M. Avramovic, P.S. Milic, O.S. Stamenkovic, V. Veljkovic, Optimization of ultrasound-assisted base-catalyzed methanolysis of sunflower oil using response surface and artificial neural network methodologies, Chem. Eng. J. 215 (2013) 82–89.
[33] M.A. Quraishi, A. Singh, V.K. Singh, D.K. Yadav, A. Singh, K Green approach to corrosion inhibition of mild steel in hydrochloric acid and sulphuric acid solutions by the extract of Murraya koenigii leaves, Mater. Chem. Phys. 122 (1) (2010) 114–122.
[34] S. Banerjee, V. Srivastava, M.M. Singh, Chemically modified natural polysaccharide as green corrosion inhibitor for mild steel in acidic medium, Corros. Sci. 59 (2012) 35–41.
[35] G. Ji, S. Anjum, S. Sundaram, R. Prakash, Musa paradisica peel extract as green corrosion inhibitor for mild steel in HCl solution, Corros. Sci. 90 (2015) 107–117.
[36] M. Srivastava, P. Tiwari, S. Kumar, R. Prakash, G. Ji, Electrochemical investigation of Irbesartan drug molecules as an inhibitor of mild steel corrosion in 1 M HCl and 0.5 M H2 SO4 solutions, J. Mol. Liq. 236 (2017) 184–197.
[37] E.S. Ferreira, C. Giacomelli, F.C. Giacomelli, A. Spinelli, Evaluation of the inhibitor effect of L-ascorbic acid on the corrosion of mild steel, Mater. Chem. Phys. 83 (1) (2004) 129–134.
[38] C. Verma, M.A. Quraishi, 2-Amino-3-methyl-3-(4-nitrophenyl)-5- (phenylthio)-3H-pyrrole-4-carbonitrile as effective corrosion inhibitor for mild steel in 1M HCl : Thermodynamical, electrochemical, surface and theoretical calculation, Ain Shams Eng. J. 7 (1) (2016) 1–9.
[39] C.B. Verma, P. Singh, I. Bahadur, E.E. Ebenso, M.A. Quraishi, Electrochemical, thermodynamic, surface and theoretical investigation of 2-aminobenzene-1, 3-di-carbonitriles as green corrosion inhibitor for aluminum in 0.5 M NaOH, J. Mol. Liq. 209 (2015) 767–778.